

Crystallinity and crystallite size measurement in polyamide and polyester fibres

A. M. Hindeleh

Department of Physics, University of Jordan, Amman, Jordan

and D. J. Johnson

Textile Physics Laboratory, Department of Textile Industries, University of Leeds, Leeds LS2 9JT, UK

(Received 13 July 1977, revised 5 September 1977)

X-ray diffraction methods for evaluating crystallinity and crystallite size in fibres generally neglect the possibility of peak overlap, and separate peaks and background by arbitrary procedures. The method described here is based on the resolution of normalized diffraction peaks in terms of combined Gaussian–Cauchy profiles for each peak, together with a polynomial background. Peak area crystallinity is then measured as the total area under the resolved peaks over a defined range. Measurements of apparent crystallite size are obtained from the widths of the resolved peaks. Application of this method to high tenacity nylon-6, nylon-6,6, and PET fibres after annealing, indicates that peak area crystallinity is about 100% for the polyamides and 85% for the polyester. The increase in apparent crystallite size is considered to be due to both an increase in the true mean size and to improvements in local lattice order.

INTRODUCTION

The state and extent of molecular order in a fibrous polymer can be assessed quite effectively by visual examination of a wide-angle X-ray diffraction photograph. Quantitative measurement of this state of order, and the size of the ordered units, usually referred to as crystallinity and crystallite size respectively, is a more difficult task, and one which has been unduly influenced by several somewhat arbitrary methods based on two phase crystalline–amorphous models of fibre structure. Here we will review methods used to measure crystallinity in thermoplastic fibres by wide-angle X-ray diffraction, and describe the application of our own procedure for the mathematical resolution of diffraction profiles including separation of the ordered and disordered parts of a diffraction trace.

The classical method of Hermans and Weidinger¹ gives an 'absolute' measure of crystallinity in terms of the ratio of the integrated intensity under the peaks to the integrated intensity under the complete trace. The major drawback to this method is the requirement that the crystalline peaks are separated from the amorphous background. Procedures for this separation, which ignore the possibility of peak overlap, are diverse: Johnson² assumed that the background in PET changes linearly between 6° and 36° (2θ) where the curve of a partly crystalline sample touches the curve of an amorphous sample; Farrow³, and Farrow and Preston⁴, used the intensity trace of an amorphous PET as a template and reduced it proportionally until it met the observed trace of a partly crystalline sample at one or two particular points; Wlochowicz and Jeziorny⁵ have constructed a separation curve based on tangents and vertical lines at various 2θ values, and Lindner⁶ and Jellinek⁷ manage to divide the PET scan into three zones corresponding to scatter from crystal-

line, intermediate, and amorphous phases. 'A new approach to the determination of crystallinity of polymers by X-ray diffraction' reported by Chung and Scott⁸ does no more than fit a mathematical function to this ubiquitous dividing line with no attempt at peak resolution. It is hardly surprising that all these methods give different 'absolute' results for crystallinity and that these values are generally low when compared with other methods for estimating crystallinity. Fortunately all the work cited above is useful in terms of relative measurements, but only with respect to one particular material and the particular method in use in the author's laboratory.

If a measure of relative crystallinity is the aim, then a more useful method of estimation is the correlation crystallinity index method introduced by Wakelin, Virgin and Crystal⁹ for use with cotton, applied to cellulose triacetate by Hindeleh and Johnson¹⁰ and to PET by Statton¹¹, and Wlochowicz and Jeziorny⁵. This method is based on the relative classification of the equatorial trace of a partly crystalline sample between the traces of two standard samples ranked with zero and 100% crystallinity. Comparison of crystallinity in thermoplastic fibres annealed at different temperatures is straightforward by this method; unfortunately comparison between specimens of different molecular type is impossible nor can estimates of crystallite size be obtained. It is of interest to note that Wlochowicz and Jeziorny find very similar results for annealed PET by the methods of Hermans and Weidinger and the correlation crystallinity index (49–51% crystallinity for a specimen annealed at 220°C). By comparison Dumbleton *et al.*¹² found the crystallinity of a PET specimen as 12% at 20°C and 33% after annealing at 240°C. Prevorsek *et al.*¹³, have obtained crystallinity values in PET allowed to contract under tension which do not exceed 60%. A comprehensive comparative

study of several methods for the evaluation of crystallinity in PET has been carried out by Gupta and Kumar¹⁴. As expected their computations show that there are considerable variations in estimates of absolute crystallinity.

The theory of paracrystallinity introduced by Hosemann¹⁵ suggests that disorder within the crystallites, caused by thermal vibrations, frozen displacements or strain, dislocations (due to chain ends), and internal distortion of the atoms, contributes to the background scatter and the breadth of each peak. Adjacent broad peaks with long tails overlap, and, by neglecting this feature, those who follow a version of the Hermans and Weidinger procedure necessarily consign a proportion of the paracrystalline scatter to the amorphous background. There have been attempts to incorporate paracrystalline scatter into the analysis; for example a rigorous approach by Ruland¹⁶ introduces a disorder function, but again separation of peaks and background is carried out in an arbitrary manner. It is hardly surprising that the existence of a paracrystalline fraction was ruled out when Ruland applied his method to a nylon specimen, or that a crystallinity value as low as 33% was reported.

The only computational methods of peak resolution reported prior to our own work were those of Fraser and Suzuki¹⁷ and Warwicker¹⁸. Both used a least squares procedure to separate peaks with Cauchy or Gaussian profiles from a linear baseline. Warwicker applied the method to both nylon-6 and nylon-6,6 annealed at different temperatures, and obtained an apparent crystallinity of 100% for all specimens. However it was pointed out that the crystallites have different amounts of lateral disorder. These findings are in direct contradiction to those of Ruland. In general, failure to separate overlapping peaks in the wide-angle X-ray diffraction pattern, and the consequent low estimates of crystallinity, have influenced conceptual models of molecular structure in thermoplastic synthetic fibres. Indeed, it is usual for models to show highly ordered regions comprising perfectly packed chain folded molecules together with a disproportionate amount of highly disordered molecules. As an example, the model depicted by Prevorsek *et al.*¹³ must be considered as a reversion to the old two phase system with a complete disregard for the concept of paracrystallinity.

It is the purpose of this paper to show that a reliable mathematical method for peak resolution, crystallinity and crystallite size measurement is available and has general application. Results are presented from several highly crystalline specimens of nylon-6,6, nylon-6 and PET, all annealed at different temperatures, together with a low crystalline PET texturized by different processes. Apart from demonstrating the practicability of the method, we hope that our results might have some bearing on models of structure.

EXPERIMENTAL

Materials

Three high tenacity yarns were used: nylon-6,6, ICI type 115 nylon; nylon-6, Courtaulds Celon and PET, ICI type 111T terylene. These yarns were annealed at constant length in a nitrogen atmosphere at various temperatures controlled to $\pm 1^\circ\text{C}$ in a range up to the melting point of each material.

Three other PET yarns have also been analysed: a conventional ICI terylene feed yarn (CONFEEED), terylene yarn texturized after drawing (CONOUT) and terylene yarn simultaneously draw-texturized (SDT). Full details of the texturizing experiments have been published elsewhere¹⁹.

X-ray diffraction

Equatorial wide-angle X-ray diffraction traces were recorded with a modified Hilger and Watts Y115 diffractometer using $\text{CuK}\alpha$ radiation from a $\gamma 90$ constant-output generator. The diffractometer output is converted via an amplifier/analyser, scaler/timer system to punched paper tape compatible with the University's 1906A computer. A typical step-scan tape would contain a fixed time count of intensity at 15 steps per degree of scattering angle, although a fixed intensity mode can be utilized if appropriate.

Correction procedure

The intensity data are averaged to 5 or 3 steps per degree as appropriate then corrected for polarization and Lorentz factors; the mean square atomic scattering factor and Compton scatter are evaluated, the incoherent scatter removed, and the coherent scatter converted to electron units by normalization of the integrated data to the integrated mean square atomic scattering factor. Output is in the form of a table of corrected intensities, a magnetic tape file of intensity in electron units, and a plot of corrected intensity against scattering angle, together with the mean square atomic scattering factor and the incoherent scatter. *Figure 1* is a typical example of graphical output exemplified by the SDT specimen.

Peak resolution

Our program for peak resolution²⁰ has been developed over a number of years and has been applied to X-ray investigations of cellulose triacetate²¹, cellulose I²² and cellulose II²³, carbon fibres²⁴ and the high performance fibres of poly(*p*-phenylene terephthalamide) (Kevlar) produced by Du Pont^{25,26}. Electron diffraction patterns have also been analysed by the same basic method^{24,26}. The program resolves multiple peak data into individual peaks and a background; it incorporates an iterative minimization procedure based on Powell's method of conjugate directions²⁷ which ensures efficient convergence of the factor S , where

$$S = \sum_{i=1}^n (Y_{(\text{obs})i} - Y_{(\text{calc})i})^2$$

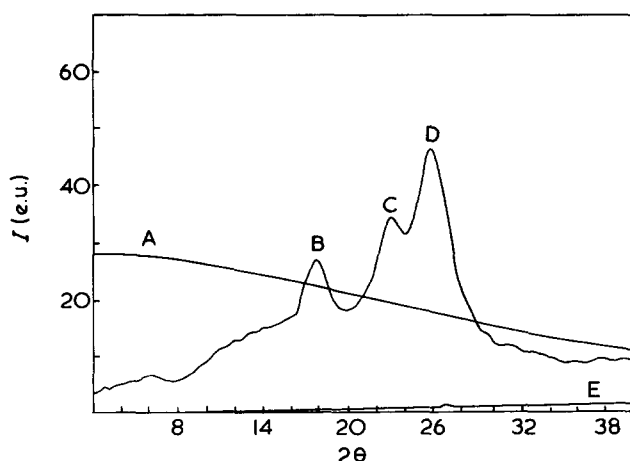


Figure 1 X-ray diffraction trace of SDT (simultaneously draw-texturized PET) after correction and normalization to electron units. A, mean square atomic scattering factor; B, 010; C, 110; D, 100; E, Incoherent scatter

for n values of $Y_{(\text{obs})}$ i.e. the corrected intensity data, and n values of $Y_{(\text{calc})}$.

$$Y_{(\text{calc})} = \sum_{t=1}^B Q_t + R$$

and

$$Q_t = f_t G_t + (1 - f_t) C_t$$

G_t is the Gaussian function

$$G_t = A_t \exp \left\{ -\ln 2 \left[\frac{2(X - P_t)}{W_t} \right]^2 \right\}$$

and C_t is the Cauchy function

$$C_t = A_t / [1 + [2(X - P_t)/W_t]^2]$$

X represents the angle 2θ .

Each peak is represented by four parameters, the profile function parameter f_t , peak height A_t , peak width W_t , and peak position P_t . Any scatter which cannot be fitted to the peaks is assigned to a background of polynomial form:

$$R = a' + b'X + c'X^2 + d'X^3$$

where a' , b' , c' , and d' are additional parameters. The program minimizes S in terms of the peak parameters and the background parameters; it is possible to constrain any of the parameters if necessary.

Choice of a Gaussian profile ($f = 1$) can be justified only for perfect crystallites of constant width; for a paracrystalline lattice, or for a distribution of crystallite size, the profile becomes more Cauchy-like ($f < 1$). A discussion of the profile function parameter f was given earlier^{21,22} and it was shown that f may take negative values in certain cases.

Peak area crystallinity

Our measure of crystallinity can be defined as a peak area crystallinity, being the ratio of the normalized scatter under the resolved peaks to the total scatter under the unresolved normalized trace. The area under the polynomial background is the non-crystalline scatter. Peak area crystallinity is arbitrarily defined between two chosen scattering angles and can best be regarded as an optimum mathematical solution.

Crystallite size

The apparent size of a crystallite normal to the planes (hkl) is given by

$$L_w(hkl) = K/ds$$

where $s = 2 \sin \theta / \lambda$, and $ds = \cos d(2\theta) / \lambda$; $d(2\theta)$ is the width in radians of the resolved peak (W). K , the Scherrer constant, is in effect a parameter of unknown value; for the purpose of simple comparison it was taken as unity both for $L_w(hkl)$ and $L_i(hkl)$. In each case the peak profile was first corrected for instrumental broadening by a program which applies a Stokes deconvolution procedure²⁸ with hexamethylene tetramine as a standard specimen. No correction for distortion broadening has been included since we have found no method which is

useful for one single order of a reflection. A detailed consideration of various methods for separating size and distortion components, and the effect on the K parameter of crystallite size distributions with known lattice distortion, has been carried out and will be reported elsewhere³¹.

Correlation crystallinity index

Standard specimens for maximum crystallinity ($C_{MAX} = 100$) and minimum crystallinity ($C_{MIN} = 0$) were prepared. In each case the C_{MAX} specimen comprised yarn annealed close to the melting point, i.e. at 210°, 250°, and 250°C for nylon-6, nylon-6,6, and PET, respectively. For the C_{MIN} standards, nylon-6 and nylon-6,6 fibrous fragments were maintained in a melted state in the capillary tube of a micro-oven specially designed to fit the X-ray diffractometer. PET fibres ball-milled for 36 h and made into a pellet at 20°C served as C_{MIN} for PET. Diffraction traces were recorded from the standard specimens and for fibres rotated in the X-ray beam. Data were analysed following a computational method used earlier in an investigation of the effect of heat treatment on the crystallinity of cellulose triacetate¹⁰.

RESULTS

High tenacity yarns

Typical output plots after peak resolution are illustrated in Figures 2–5; Figure 2 is nylon-6, as received, depicting the equatorial trace resolved into two peaks, 200 and 202,002, together with a background curve; Figure 3 is nylon-6,6 annealed at 170°C and resolved into two peaks 100 and 110,010, plus background; Figure 4 is PET, as received; Figure 5 is PET, annealed at 250°C, both resolved into 010, 110, and 100 peaks together with the background. A selection of the most significant characterization parameters derived from the resolution and deconvolution programs are given in Table 1; in this work, the peak area crystallinity was measured in the range 10° to 34° (2θ). Additional measurements showed that there were no significant differences in orientation on annealing.

Three important points can be elaborated:

(i) The background scatter in these high tenacity yarns is very low, both nylon-6 and nylon-6,6 approach 100% peak area crystallinity in the range above, whereas a reasonable

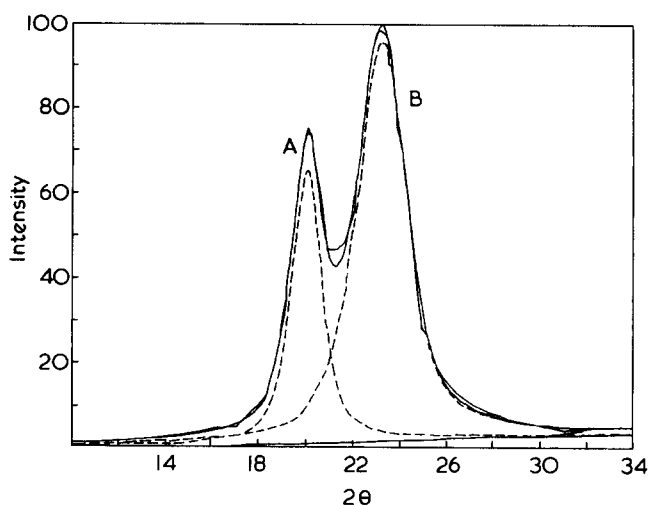


Figure 2 Nylon-6 (20°C), as received, normalized equatorial diffraction trace together with best-fit calculated intensity and its resolution into two peaks and a background. A, 200; B, 202, 002

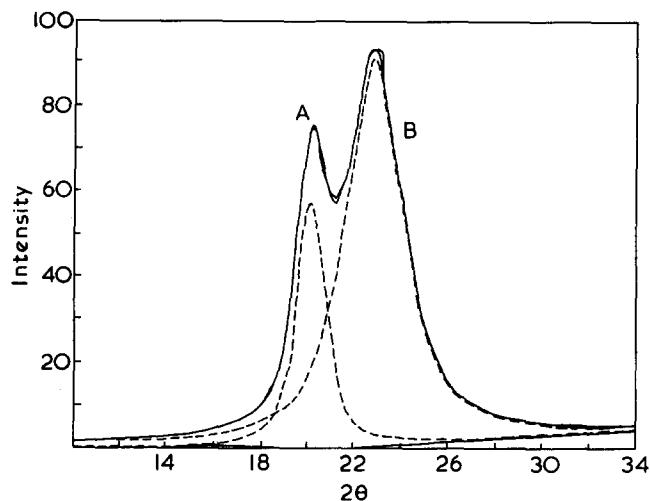


Figure 3 Nylon-6,6 (170°C), annealed at 170°C, normalized equatorial diffraction trace together with best-fit calculated intensity and its resolution into two peaks and a background. A, 100; B, 110, 010

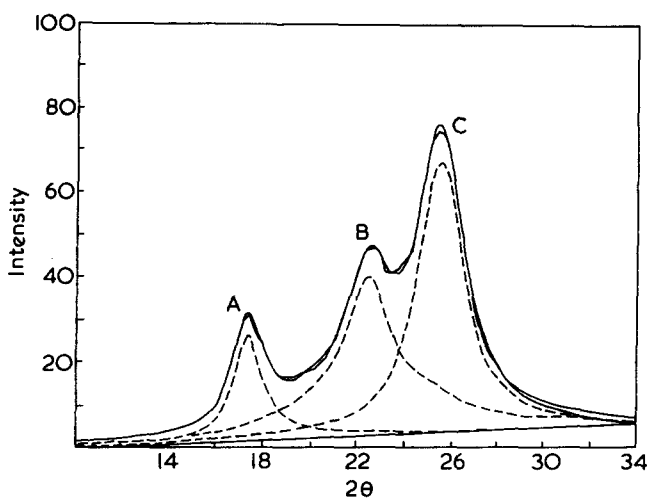


Figure 4 PET (20°C), as received, normalized equatorial diffraction trace together with best-fit calculated intensity and its resolution into three peaks and a background. A, 010; B, 110; C, 100

mean value for PET may be considered as 85%. By way of comparison, a nylon-6,6 monofilament was found to have a crystallinity of 72%, and a PET yarn for textile purposes had a crystallinity of 64%. The error in measuring peak area crystallinity has been estimated at around 5%²⁹.

(ii) The typical increase in peak height and concomitant decrease in peak width found on annealing, are clearly illustrated in Figures 4 and 5. The decrease in peak width, an apparent indication of the increase in crystallite size, is not significant until the annealing temperature exceeds 200°C in the case of PET, 180°C in the case of nylon-6, and 170°C for nylon-6,6.

(iii) The correlation crystallinity index reveals an initial drop in the relative crystallinity of each specimen which increases on annealing above the temperatures quotes in (ii). The initial fall in crystallinity, as measured by this method, suggests that frozen-in strains are released upon annealing and give a slightly more disordered system than the original fibre, which will have been treated during production to a temperature around that given in (ii), but for a relatively short period of time.

Texturized PET

A full discussion of these materials has been reported¹⁹ but it is useful to include the X-ray diffraction results here since they presented a much more difficult problem than the high tenacity fibres because of the lower overall crystallinity. Figure 6 illustrates peak resolution in the simultaneously draw-texturized yarn SDT; the peaks are considerably less sharp than in the high tenacity PET and there is a greater

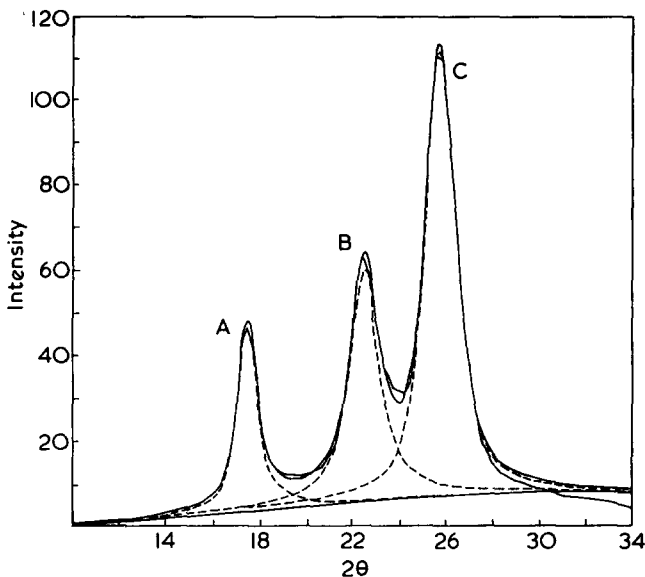


Figure 5 PET annealed at 250°C, normalized equatorial diffraction trace together with best-fit calculated intensity and its resolution into three peaks and a background. A, 010; B, 110; C, 100

Table 1 X-ray characterization parameters after peak resolution of annealed PET, nylon-6,6 and nylon-6

Specimen	Annealing temperature (°C)	Correlation crystallinity (%)	Peak area crystallinity (%)	Crystallite size (nm)			Peak height (e.u.)			
				(010)	(110)	(100)	(010)	(110)	(100)	
PET	20	71	88	5.9	3.4	3.9	25	37	62	
	100	67	88	5.8	3.5	3.9	25	38	67	
	200	73	84	6.6	5.1	4.2	29	45	79	
	250	100*	83	9.6	6.2	6.0	43	54	104	
				Crystallite size (nm)			Peak height (e.u.)			
				(100)	(110 + 010)	(100)	(110 + 010)			
Nylon-6,6	20	82	100	6.3	3.1	55	94			
	170	83	96	6.3	3.0	57	90			
	250	100*	100	7.1	4.4	65	113			
				Crystallite size (nm)			Peak height (e.u.)			
				(200)	(202 + 002)	(200)	(202 + 002)			
Nylon-6	20	90	92	6.0	3.6	66	94			
	180	84	100	7.3	3.9	72	103			
	210	100*	100	8.8	4.6	89	118			

* CMAX standard specimen

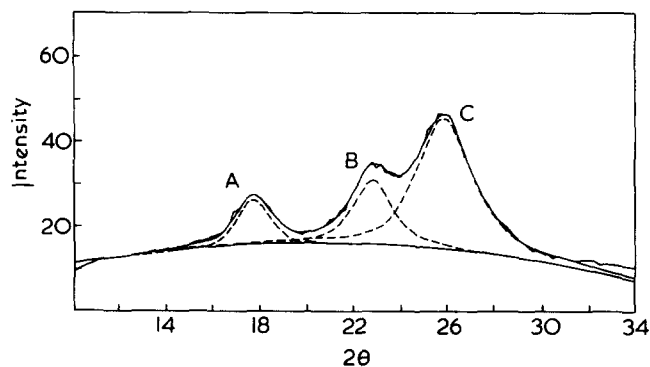


Figure 6 Simultaneously draw-texturized PET yarn (SDT), normalized equatorial diffraction trace (see Figure 1) together with best-fit calculated intensity and its resolution into three peaks and a background. A, 010; B, 110; C, 100

background scatter. Table 2 gives some relevant information from the peak resolution output; in particular the peak area crystallinity is only half that of the high tenacity PET. The background curve was only found successfully for these three specimens after including a fourth peak of very broad profile and adding this to the background after resolution. The slight drop in crystallinity between the CONFEEED specimen and the two draw-texturized specimens may be just significant as may be the fall in intensity of the 100 reflection. Evidently the different methods of texturizing have little effect on fine structure apart from a slight decrease in order of the chain molecules.

DISCUSSION

Crystallinity measurement

This investigation has proved that all samples of nylon and PET exhibit considerable overlap of the diffraction peaks and that peak resolution is the only valid method to obtain reliable parameters for the measurement of apparent crystallite size and peak area crystallinity. However, indications of small changes of crystallinity in a series of specimens of the same type are best found by the correlation crystallinity method. For the comparison of reasonably different specimens of the same type, for specimens of a different type, or for comparisons between different specimens or different laboratories, then the peak area crystallinity is a very useful characterization parameter.

Polyamides

There is practically no change in the peak area crystallinity upon annealing the high tenacity polyamide specimens close to the melting point, but there is a significant increase in amplitude and decrease in width or integral breadth of the resolved peaks. This phenomenon can be attributed to improvement in lattice order and/or increase in the size of the scattering crystallites; it has nothing to do with changes in orientation, which are negligible. If we temporarily discount an increase in lattice order, then the increase in apparent crystallite size in the direction of the hydrogen bonded planes, 002 in nylon-6 and 010 in nylon-6,6, as given by measurements on the 200 and 100 reflections respectively, amounts to 47% in nylon-6 and 13% in nylon-6,6. In the direction of packing of the hydrogen bonded sheets, the increase in apparent crystallite size is about 30% in both polyamides, as measured from the 202 + 002 (nylon-6) and 110 + 010

(nylon-6,6) reflections. Although the extent of the crystallites parallel to the hydrogen-bonded sheets is approximately double that of the extent in the direction of packing of the crystallites, there is no significant evidence for preferential growth in either direction. This result suggests that an increase in crystallite size may not be the only cause of the changes in peak parameters on annealing.

Evidence from electron micrographs showing images of crystallites in cellulose triacetate²¹, in carbon fibres³⁰, and in PPT fibres²⁶, proves that annealing or other changes in crystallization conditions can lead to a real increase in crystallite size in terms of the mean value of a somewhat skewed size distribution. Studies of lattice-fringe images in carbon fibres show that an increase in crystallite size is usually accompanied by an improvement in the lattice order. The Scherrer parameter (held constant at 1 here), which may best be considered as the ratio of true size to apparent size, has been shown in recent work to be a function of lattice order³¹. Consequently, until lattice order can be assessed by a reliable method, the true crystallite size will remain indeterminate. Although the quantitative results given here are substantially in agreement with those of Warwicker¹⁸, we must disagree with his verdict that the decrease in peak width on annealing is entirely due to an increase in lattice order. Our conclusion is that there is both an increase in mean crystallite size and an increase in the local lattice order (the lattice order of the first kind as defined by Hosemann).

The lack of significant change in the peak area crystallinity of the high-tenacity polyamides on annealing indicates that there are no changes in long range lattice order, i.e. that of the second kind as defined by Hosemann. However, other specimens do show changes in peak area crystallinity on annealing, for example a series of nylon-6 tapes showed an increase from 57 to 79% with little change in peak width. This result indicates a real increase in the ordered (crystalline) phase at the expense of the disordered (amorphous) phase.

Since this work was carried out, Huismann, Heuvel and Lind³² have reported the use of a peak resolution program to separate the α and γ fractions of nylon-6. Their program is based on a Pearson function which is very similar to the combined Gaussian-Cauchy function used here. Unfortunately, recent tests showed that, because their shape parameter becomes infinite for a Gaussian profile, its use in our program is computationally difficult. The results are not significantly different, and indeed we had previously tested our specimens for the presence of a γ phase by attempting resolution with a third peak. Peak resolution always gave a negligible third peak and we concluded that our specimens had no γ phase. Nevertheless, it would seem reasonable to suggest that all peak resolution of equatorial X-ray diffraction traces of nylon-6 should be carried out with the possibility of a third peak incorporated.

Table 2 X-ray characterization parameters after peak resolution of texturized PET: CONFEEED, conventional feed yarn, CONOUT, conventionally texturized yarn, SDT, yarn simultaneously draw texturized

Specimen	Peak area crystallinity (%)	Crystallite size (nm)			Peak height (e.u.)		
		(010)	(1 $\bar{1}$ 0)	(100)	(010)	(1 $\bar{1}$ 0)	(100)
CONFEEED	46	5.1	3.9	3.1	11	15	37
CONOUT	39	5.2	3.8	3.3	12	15	34
SDT	37	5.4	4.3	3.3	11	15	31

Polyesters

We have investigated polyester specimens of both high and low crystallinity. On our absolute scale the value of 85% quoted for the high tenacity PET is the highest obtained with this material, other PET specimens examined here have given peak area crystallinities in the 35 to 70% range. Evidently there is always a disordered phase associated with PET fibres. Despite the lack of significant change in peak area crystallinity when high tenacity yarn is annealed close to the melting point, there is a significant increase in height and decrease in width of the resolved profiles. Once again these changes can best be interpreted in terms of a real increase in the mean size of the crystallite size distribution with a concomitant improvement in the local lattice order.

Fischer and Fakirov³³ have recently studied the wide-angle X-ray scattering of annealed PET bristle; they assume that since there are no changes in lattice spacing with annealing temperature there are no paracrystalline distortions in the crystallites, and that crystallite size broadening predominates. Whilst we agree that crystallite sizes are indeed increasing on annealing, recent theoretical work shows that even 5% distortion gives little significant change in lattice spacing. The method of measurement of lattice spacing must also be questioned since only after peak resolution can the true peak position be found. Fischer and Fakirov have also performed a very detailed analysis of the small-angle scattering of PET bristles. They find the usual increase of intensity in the meridional scatter on annealing, and attribute this to an increase in crystalline density although overall crystallinity is not changed. Having excluded paracrystalline distortions from their crystallites, they assume lattice vacancies at grain boundaries and support a mosaic-block model of structure. It is interesting to note that polyamide tapes and polyester bristles show a perfectly clear equatorial small-angle scatter; the weak equatorial scatter observed with fibres can be attributed to multiple scatter from the fibres themselves. There is consequently no indirect evidence for discrete microfibrils or any crystallite void system. The crystallites must be well packed with no appreciable density difference between them.

In the absence of the type of direct observations we have been able to make on carbon and PPT fibres by high resolution electron microscopy, there can be no definite structural conclusions about any form of PET. However, it would seem that high tenacity PET has a distribution of well packed crystallites incorporating some lateral disorder of the first kind and with the disorder of the second kind being confined to chain folded regions along the fibre. Annealing improves the mean crystallite size, the local disorder, and the longitudinal order. Specimens with a lower peak area crystallinity will have a more well defined disordered phase; this could give rise to the type of pseudo-fibrillar structure observed by Reimschuessel and Prevorsek³⁴ after staining. Consideration of their observations on both polyamide and polyester specimens must be deferred until it can be proved that the electron beam has no effect on the disposition of the stain and that cutting has had no effect on the structure of the sections.

Finally we must comment that there are no indications of the presence of an intermediate phase in the PET specimens examined here.

CONCLUSIONS

Resolution of a normalized X-ray trace into peaks and background, with each peak described in terms of peak height,

width, position and profile, by means of a combined Gaussian—Cauchy function, provides the best mathematical method for crystallinity estimation. Peak area crystallinity can be evaluated between any given limits as a parameter with a precisely defined mathematical significance. The resolved peak widths can be corrected for instrumental broadening to give estimates of apparent crystallite size.

Increases in apparent crystallite size for both polyamide and polyester specimens are considered to be the result of both a real increase in mean size and an improvement in local lattice order. Models of fine structure in thermoplastic fibres must take into account the thermal history of the specimen; they will inevitably remain somewhat speculative until reliable direct observations by electron microscopy are possible.

ACKNOWLEDGEMENTS

A. M. H. thanks the University of Jordan and the Jordan Science Research Council for financial support. We thank P. E. Montague for testing the effectiveness of a Pearson type function.

REFERENCES

- 1 Hermans, P. H. and Weidinger, A. *Text. Res. J.* 1961, **31**, 558
- 2 Johnson, J. E. *J. Appl. Polym. Sci.* 1959, **5**, 205
- 3 Farrow, G. *Polymer* 1960, **1**, 518; 1961, **2**, 409
- 4 Farrow, G. and Preston, D. *Br. J. Appl. Phys.* 1960, **11**, 353
- 5 Wlochowicz, A. and Jeziorny, A. *J. Polym. Sci. (A-2)* 1972, **10**, 1407
- 6 Lindner, W. L. *Polymer* 1973, **14**, 9
- 7 Jellinek, G. Personal communication
- 8 Chung, F. H. and Scott, R. W. *J. Appl. Crystallogr.* 1973, **6**, 225
- 9 Wakelin, J. H., Virgin, H. S. and Crystal, E. *J. Appl. Phys.* 1959, **30**, 1654
- 10 Hindeleh, A. M. and Johnson, D. J. *Polymer* 1970, **11**, 666
- 11 Statton, W. O. *J. Appl. Polym. Sci.* 1963, **7**, 803
- 12 Dumbleton, J. H., Buchanan, D. R. and Bowles, B. B. *J. Appl. Polym. Sci.* 1968, **12**, 2067
- 13 Prevorsek, D. C., Tirpak, G. A., Harget, P. J. and Reimschuessel, A. C. *J. Macromol. Sci. (B)* 1974, **9**, 733
- 14 Gupta, V. B. and Kumar, S. *Indian J. Text. Res.* 1976, **1**, 72
- 15 Hosemann, R. and Bagchi, S. N. 'Direct Analysis of Diffraction by Matter', North Holland, Amsterdam, 1962, p 656
- 16 Ruland, W. *Acta Crystallogr.* 1961, **14**, 1180
- 17 Fraser, R. D. B. and Suzuki, E. *Anal. Chem.* 1966, **38**, 1771
- 18 Warwicker, J. O., *J. Soc. Dyers Colour.* 1970, **86**, 303
- 19 Tucker, P., Johnson, D. J., Dobb, M. G. and Sikorski, J. *Text. Res. J.* 1977, **47**, 29
- 20 Hindeleh, A. M. and Johnson, D. J. *J. Phys. (D)* 1971, **4**, 259
- 21 Hindeleh, A. M. and Johnson, D. J. *Polymer* 1972, **13**, 27
- 22 Hindeleh, A. M. and Johnson, D. J. *Polymer* 1972, **13**, 423
- 23 Hindeleh, A. M. and Johnson, D. J. *Polymer* 1974, **15**, 697
- 24 Bennett, S. C., Johnson, D. J. and Montague, P. E. *Proc. Fourth London Int. Carbon and Graphite Conf.* 1974 p 503
- 25 Dobb, M. G., Hindeleh, A. M., Johnson, D. J. and Saville, B. P. *Nature* 1975, **253**, 189
- 26 Dobb, M. G., Johnson, D. J. and Saville, B. P. *J. Polym. Sci.* to be published
- 27 Powell, M. J. D. *Comput. J.* 1964, **7**, 155
- 28 Stokes, A. R. *Proc. Phys. Soc. (A)* 1948, **61**, 382
- 29 Montague, P. E. *M. Phil. Thesis*, University of Leeds, (1975)
- 30 Bennett, S. C., Johnson, D. J. and Murrey, R. *Carbon* 1976, **14**, 117
- 31 Johnson, D. J. and Montague, P. E. to be published
- 32 Heuvel, H. M., Huisman, R. and Lind, K. C. J. B. *J. Polym. Sci. (Polym. Phys. Edn)* 1976, **14**, 921
- 33 Fischer, E. W. and Fakirov, S. *J. Mater. Sci.* 1976, **11**, 1041
- 34 Reimschuessel, A. C. and Prevorsek, D. C. *J. Polym. Sci. (Polym. Phys. Edn)* 1976, **14**, 485